Quasi-static Modal Analysis based on Implicit Condensation for Structures with Nonlinear Joints

M.S. Allen[1], **R.M. Lacayo**[1], **& M.R.Brake**[2]
[1] University of Wisconsin-Madison, Engineering Physics Department
1500 Engineering Drive, Eng. Research Building
Madison, WI, 53706, USA
email: **msallen@engr.wisc.edu, rmlacay@hotmail.com**

[2] Sandia National Laboratories*
P.O. Box 5800, Albuquerque, NM, 87185, USA
email: **mrbrake@sandia.gov**

Abstract

Significant insight can be gained into the dynamics of a structure with bolted interfaces by observing the change in the effective modal natural frequency and damping of each mode of the structure as excitation amplitude increases. Unfortunately, current methods for estimating these parameters require that the model be integrated through several dynamic transient simulations at considerable computational expense. Festjens, Chevallier and Dion [Int. J. Mech. Sci. 75:170-177, 2013] recently proposed an alternative based on quasi-static analysis. This work builds on theirs, presenting an alternate derivation and alternative means of extracting the frequency and damping. The utility of the approach is then explored by using it to estimate the modal frequency and damping of two structures where bolted interfaces are modeled using discrete Iwan joints. The cases studied show that the methodology is highly effective in the micro-slip regime and provides several orders of magnitude reduction in the computational cost.

1 Introduction

Much of the uncertainty in finite element models for built up structures comes from the interfaces (e.g. bolted, riveted, press-fit, etc…). They are also a major source of damping and can often behave nonlinearly; see [1] and [2] for a review of these issues. Improved methods for modeling joints have been presented recently, and when coupled with substructuring methods it is beginning to be possible to model realistic structures including the damping and nonlinearity from Coulomb friction at the interface. For example, see the harmonic balance methods in [3] and [4]. However, these methods can still be very expensive and none of the joint modeling paradigms has been thoroughly validated against measurements. In many cases the joints behave almost linearly in terms of the stiffness and mass, while exhibiting strong damping nonlinearities. Because damping is typically light (i.e. a second order effect), it seems reasonable to seek approaches that use these facts to simplify modeling and simulation. For example, recent works have shown that, when the joints remain in the micro-slip regime, some structures can be modeled effectively as a superposition of weakly nonlinear single-degree-of-freedom oscillators [5-7]; one can use this to create a highly efficient reduced order model to predict the response of the structure.

It is generally accepted that interfaces behave quasi-statically, but there is a disconnect between the behavior of joints, which has been studied extensively in the contact mechanics community (see, e.g. [8,

*Sandia is a multi-program laboratory operated by Sandia Corporation, a Lockheed Martin Company, for the United States Department of Energy's National Nuclear Security Administration under Contract DE-AC04-94AL85000.

9]) and the effect on the dynamic response. One recent work by Festjens, Chevallier & Dion [10] sought to overcome this by enforcing the modal motion as a boundary condition on a detailed, nonlinear quasi-static model for the region around the joints. They proposed a method that could be used to adjust the mode shapes near the joint as amplitude increases, to account for the slight softening that occurs near the joints. Their methodology was found to provide good estimates of the effective damping and natural frequency of a cantilever beam with a bolted joint near its root, when compared to a full order nonlinear dynamic simulation of the whole structure including Coulomb friction at the joint interface.

This work builds on that of [10, 11] in a few ways. First, the derivation presented here focuses on applying a quasi-static force that deforms the structure in the same way in which it would deform dynamically, and the resulting response is used to estimate a reduced order model that uses the linearized modes as basis vectors. In essence, we show that this method is an extension of the Implicit Condensation and Expansion method [12, 13] (also see [14]) to structures with damping. In contrast, in [10, 11] Festjens et al. apply a combination of boundary conditions and static loads to the region around the joint, which may obscure this point. The derivation presented here explains that, because a force is applied rather than a displacement, the structure is free to adjust quasi-statically in response to small changes in the stiffness near the joint. As a result, it is not necessary to include basis vectors associated with those small changes in the displacement field near the joint. In the end the comparison reveals that the method proposed here is a special case of one of the methods in [10, 11]. Second, the method proposed in this paper does not seek to update the mode shape with displacement amplitude as was done in [10, 11], so it is somewhat simpler, and the simulation results show that outstanding results can still be obtained in the regime of interest. Finally, whereas Festjens et al. were concerned with high fidelity models where Coulomb friction was assumed to hold at the contact interface, this work focuses on structures where the joints are modeled with a single discrete 4-parameter Iwan joint for each interface [15]. These Iwan models have been validated over a large range of response amplitude, spanning the microslip regime [2] and hence the performance of the modal approach can be quantified over a large range of response amplitude.

The rest of this paper is organized as follows. The following section presents the theory behind the proposed method and discusses similarities with the method in [10, 11]. Section 3 demonstrates the method on a simple mass spring system, and Section 4 presents the results when the method is applied to a finite element model of two beams that are joined by four bolts, similar to the hardware that was tested in [16] and simulated in [16], i.e. the "Sumali Beam." Section 5 presents the conclusions.

2 Theoretical Development

Consider an otherwise linear structure that contains localized nonlinearities due to the joints that, in the most general case, could depend on the displacements $\mathbf{x}$ and velocities $\dot{\mathbf{x}}$ as well as on internal states $\boldsymbol{\theta}$ within the joint model. (For example, internal slider states are used in the Iwan formulation [15]). The joint model manifests iself as a vector of nonlinear forces $\mathbf{f}_J$ within the system equations of motion as follows

$$\mathbf{M}\ddot{\mathbf{x}} + \mathbf{C}\dot{\mathbf{x}} + \mathbf{K}\mathbf{x} + \mathbf{f}_J(\mathbf{x}, \dot{\mathbf{x}}, \boldsymbol{\theta}) = \mathbf{f}_{ext}(t) \tag{1}$$

For small vibrations, one can define a linear system that approximates the response about some equilibrium,

$$\mathbf{M}\ddot{\mathbf{x}} + \mathbf{C}\dot{\mathbf{x}} + \left(\mathbf{K} + \nabla\mathbf{f}_J\big|_{\mathbf{x}_0}\right)\mathbf{x} = \mathbf{f}_{ext}(t) \tag{2}$$

where $\nabla\mathbf{f}_J\big|_{\mathbf{x}_0}$, denotes the Jacobian of the nonlinear forces at the equilibrium state $\mathbf{x}_0$. One can now solve an eigenvalue problem to find the system's natural frequencies, ω_{0r}, and mass-normalized mode shapes $\boldsymbol{\varphi}_{0r}$ about this reference state:

$$\left[\left(\mathbf{K} + \nabla\mathbf{f}_J\big|_{\mathbf{x}_0}\right) - \omega_{0r}{}^2\mathbf{M}\right]\boldsymbol{\varphi}_{0r} = 0 \tag{3}$$

Physically, Eq. (3) produces the modal properties of the system at very low response amplitudes when the joints are stuck. One must take care not to confuse these modal properties with those of the structure when all joints slip completely, which occurs at very high response amplitudes. The high-amplitude properties are computed with

$$\left[\mathbf{K} - \omega_{\infty r}{}^2 \mathbf{M}\right] \boldsymbol{\varphi}_{\infty r} = 0 \tag{4}$$

The system in Eq. (1) can be transformed to modal coordinates using the low-amplitude modal basis of the structure. Traditionally, this is done using the transformation $\mathbf{x} = \boldsymbol{\Phi}_0 \mathbf{q}$, where $\boldsymbol{\Phi}_0 \in \mathbb{R}^{N \times m}$ and $m<<N$, is the matrix of mode shape vectors $\boldsymbol{\varphi}_{0r}$. This produces the following equation of motion for mode r:

$$\ddot{q}_r + 2\zeta_{0r}\omega_{0r}\dot{q}_r + \boldsymbol{\varphi}_{0r}^{\mathrm{T}}\mathbf{K}\boldsymbol{\varphi}_{0r} q_r + \boldsymbol{\varphi}_{0r}^{\mathrm{T}}\mathbf{f}_J(\mathbf{x}, \dot{\mathbf{x}}, \boldsymbol{\theta}) = \boldsymbol{\varphi}_{0r}^{\mathrm{T}}\mathbf{f}_{ext}(t) \tag{5}$$

Equation (5) assumes that the modes diagonalize the linear damping so the low-amplitude linear damping ratio has been defined in terms of the low-amplitude frequency using $\zeta_{0r} = \boldsymbol{\varphi}_{0r}{}^{\mathrm{T}}\mathbf{C}\boldsymbol{\varphi}_{0r} / (2\omega_{0r})$. This also assumes that the joints do not induce any additional damping at low energy.

2.1 General Formulation for Nonlinear Forces

If we apply the well known Ritz/Galerkin approach to the equation of motion, then the nonlinear joint forces would be written as follows,

$$\boldsymbol{\varphi}_{0r}^{\mathrm{T}}\mathbf{f}_J(\mathbf{x}, \dot{\mathbf{x}}, \boldsymbol{\theta}) = \boldsymbol{\varphi}_{0r}^{\mathrm{T}}\mathbf{f}_J(\boldsymbol{\varphi}_0\mathbf{q}, \boldsymbol{\varphi}_0\dot{\mathbf{q}}, \boldsymbol{\theta}) \tag{6}$$

where the displacements $\mathbf{x} = \boldsymbol{\varphi}_0\mathbf{q}$ are now required to be spanned by the modes of the linearized system. This is known to be inadequate for geometrically nonlinear problems [12-14], and it proves problematic here as well. The joints undergo microslip in the region very close to a joint, and as a result very many modes must be included before the term $\boldsymbol{\varphi}_0\mathbf{q}$ can describe the displacement adequately in the region very close to the joints.

The first step in the traditional ICE method [12-14] is to assume that the nonlinear term can be approximated as follows, which is exactly the same form as used in the traditional Ritz/Galerkin method.

$$\mathbf{g}(\mathbf{q}) \approx \boldsymbol{\Phi}_0{}^{\mathrm{T}}\mathbf{f}_J(\mathbf{x}) \tag{7}$$

However, rather than assume that the displacements are well represented by $\mathbf{x} = \boldsymbol{\varphi}_0\mathbf{q}$, in the ICE method we instead apply a set of quasi-static loads $\mathbf{M}\boldsymbol{\varphi}_{0r}$ to the finite element model and then fit a model of the form $\mathbf{g}(\mathbf{q})$ to the load displacement data. The nonlinearities are assumed to depend on displacements alone and the rth row of the nonlinear function is typically approximated as

$$g_{r,\mathrm{ICE}}(\mathbf{q}) = \sum_{i=1}^{m}\sum_{j=i}^{m} B_r(i,j) q_i q_j + \sum_{i=1}^{m}\sum_{j=i}^{m}\sum_{k=j}^{m} A_r(i,j,k) q_i q_j q_k \tag{8}$$

Using this approach, the structure is allowed to relax into any of its modes during the quasi-static loading, and the model simply captures the projection of the resulting forces onto the reduced basis. Hence, the effect of all higher order modes is capture implicitly. This approach could be extended to the present formulation, and in future works it will be pursued in case coupling between the linear modes must be captured, but the remainder of this paper will pursue a simpler approach instead.

2.2 Formulation in Terms of Uncoupled Nonlinear Oscillators

Empirical evidence [6, 7, 17] suggests that the linear modes tend to be preserved for a structure with typical nonlinearities due to bolted interfaces, so that one can approximate the response effectively with a superposition of weakly nonlinear oscillators. The theoretical foundation for such an occurrence is detailed in [18]. When such a model is appropriate, then the nonlinear function for the *r*th mode is a scalar and the nonlinear forces are approximated as follows.

$$\mathbf{g}(\mathbf{x}, \dot{\mathbf{x}}, \boldsymbol{\theta}) = \begin{bmatrix} \ddots \\ g_r(q_r, \dot{q}_r, \boldsymbol{\theta}) \\ \ddots \end{bmatrix} \tag{9}$$

We next assume that the nonlinear forces are independent of velocity, and that each mode obeys the Masing assumptions, which are outlined in [15, 19] and allow the hysteresis curve to be constructed from a single loading. Specifically, the following symmetries are assumed to exist:

- The "forward" part of the hysteresis curve will look like the loading ("backbone") curve, but stretched along each of the displacement and force axes by a factor of two and translated to terminate at the tip of the backbone curve.
- The "return" part of the hysteresis curve will look like the forward part, but reflected along each of the displacement and force axes.
- The equation of any hysteretic response curve is obtained by 1) applying the Masing hypothesis using the latest point of loading reversal and 2) requiring that if an active curve crosses a curve described in a previous cycle, the current curve follows that of the previous cycle.

These assumptions were derived for a single joint (or a single deformation mode of a plastic material in the early works by Masing) but in this work we shall assume that this holds for each mode of vibration. Specifically, we excite each mode in turn with a force applied over the entire structure in the shape of that linear mode by solving the following quasi-static problem,

$$\mathbf{K}\mathbf{x} + \mathbf{f}_J(\mathbf{x}, \boldsymbol{\theta}) = \mathbf{M}\boldsymbol{\varphi}_{0r}\alpha \tag{10}$$

where α is the load amplitude. This produces the quasi-static response $\mathbf{x}$ of the structure up to some maximum load amplitude. The response is written to file at several intermediate steps to obtain the entire load displacement curve. The resulting displacements are then mapped to each of the modes using $q_r(\alpha) = \boldsymbol{\varphi}_{0r}{}^{\mathrm{T}}\mathbf{M}\mathbf{x}(\alpha)$. The modes that were not directly excited are also retained and used to assess the degree to which the modes are statically coupled at each load amplitude. It is also important to note that we have obtained a single valued relationship between $\mathbf{x}(\alpha)$ and α by requiring that the load always ramp from an unloaded state to a maximum load α_{max}. As a result, it is no longer necessary to track any internal states, $\boldsymbol{\theta}$.

One can now use the curve of the modal force $f_r(\alpha) = \boldsymbol{\varphi}_{0r}{}^{\mathrm{T}}\mathbf{M}\boldsymbol{\varphi}_{0r}\alpha = \alpha$ versus modal displacement q_r to construct the full hysteresis curve using Masing's rules, as shown in Fig. 1.

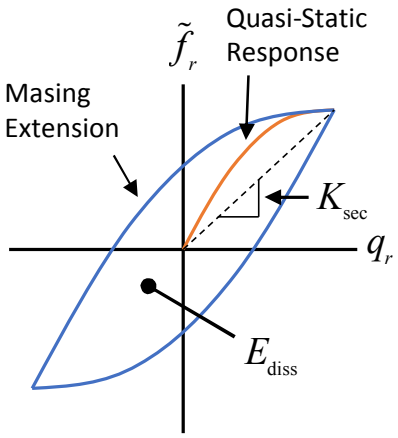

Figure 1: (red) Sample loading curve obtained by solving Eq. (10). (blue) Hysteresis curve (forward and reverse) computed using Masing's rules.

Hysteresis curves such as these can now be used to estimate the instantaneous stiffness and damping for each mode. Specifically, the secant to the curve is used to define the stiffness, as follows.

$$\omega_r(\alpha) @ \sqrt{\frac{f_r(\alpha)}{q_r(\alpha)}} \tag{11}$$

The energy dissipated per cycle of vibration is the area enclosed by the full hysteresis curve

$$\begin{aligned} D_r(\alpha) &= \int_{-q_r(\alpha)}^{q_r(\alpha)} \left(2f_r - f_r(\alpha)\right) dq_r + \int_{q_r(\alpha)}^{-q_r(\alpha)} \left(-2f_r + f_r(\alpha)\right) dq_r \\ D_r(\alpha) &= 2\int_{-q_r(\alpha)}^{q_r(\alpha)} \left(2f_r - f_r(\alpha)\right) dq_r \end{aligned} \tag{12}$$

where it should be understood that $f_r(\alpha)$ is the constant maximum load at the level, α, of interest, and f_r is a function of displacement q_r. This simplifies to four times the integral of the nonlinear part of the force displacement curve, as explained in [10]. In this work this integral is evaluated numerically using trapezoidal integration based on a certain number of samples N_α samples of $f_r(\alpha)$ and $q_r(\alpha)$ along the loading curve.

Then, using the relationship between energy dissipated per cycle and the damping ratio (for a linear system), the effective damping ratio can then be calculated from the following.

$$\zeta_r(\alpha) = \frac{D(\alpha)}{2\pi \left(q_r(\alpha)\omega_r(\alpha)\right)^2} \tag{13}$$

2.2.1 Comparison with the FCD method in [10].

The proposed method is quite similar to that presented by Festjens, Chevallier and Dion in [10], and which shall be denoted the FCD method here. They proposed to divide the structure into two portions: a nonlinear domain (a), which includes the area near the joints, and a linear domain (b) composed of the rest of the structure. They then solve the following quasi-static problem, which includes the inertial load due to motion of domain (a) and loads due to the deformation of domain (b). The latter probably dominates in many problems.

$$\mathbf{K}_{aa}\mathbf{u}_a + \mathbf{f}_J(\mathbf{u}_a) = \left(\omega^2 \mathbf{M}_{aa}\boldsymbol{\varphi}_{ar} - \mathbf{K}_{ab}\boldsymbol{\varphi}_{br}\right)\alpha \tag{14}$$

They then present two updating schemes that can be used to adjust the mode shapes to accommodate the small changes in the mode shapes that occur near the joints. The approach presented here is identical to their approach if 1) the nonlinear domain is extended to include the entire structure and 2) the mode shapes are not updated with amplitude. The definitions of instantaneous damping and instantaneous natural frequency used here are also slightly different than those that they used.

2.3 Hilbert Fitting Methods

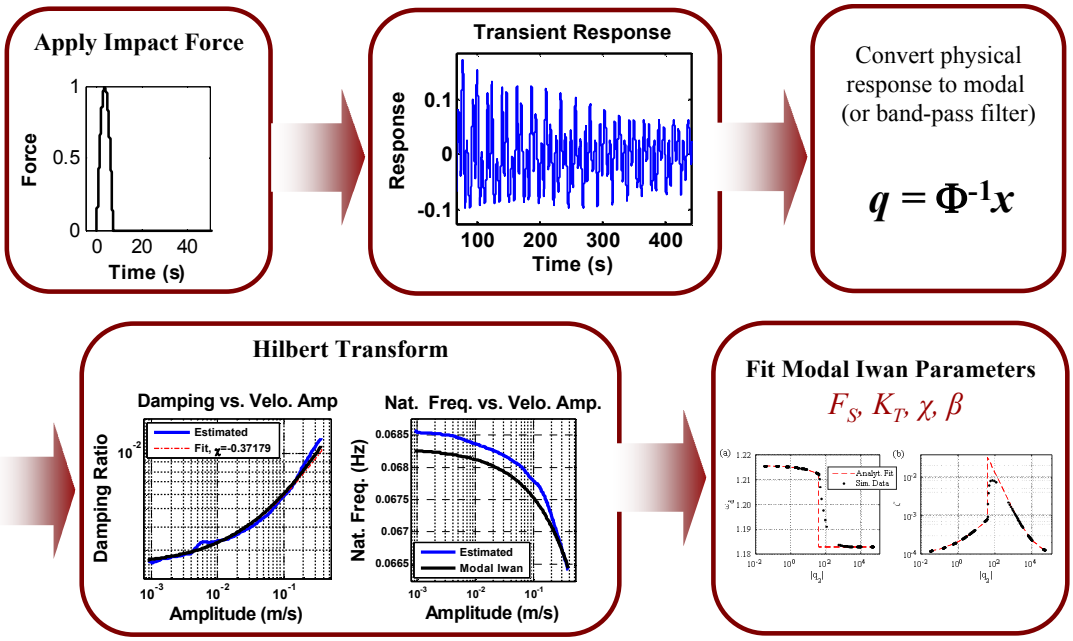

Figure 2: Flowchart describing the method used in [6, 7] to estimate the parameters of uncoupled modal models (or modal Iwan models) from a physical model with discrete joints.

The proposed quasi-static method will be validated by comparing it with the technique developed by the authors in [6, 7, 16]. As summarized in Figure 2, the dynamic response of the structure to an impulsive load is found, separated into modal contributions, and then a Hilbert transform is used to extract the instantaneous natural frequency and damping ratio for each mode. This approach also reveals whether modal couplings are significant, as explained in [7, 16].

For the results presented here, the impulsive load was shaped so as to maximize the contribution of each mode in turn. Specifically, Eq. (1) is integrated subject to the following impulsive force,

$$\mathbf{f}_{ext}(t) = \mathbf{M}\boldsymbol{\varphi}_{0r} p \sin(\omega_{0r} t), \quad t < \pi/\omega_{0r}\,, \tag{15}$$

where p is a scalar multiplier to change the load amplitude. In [7, 16] impulses are applied at points and those results are compared to this special case; see those works for further details. In the results that follow, the time response of a particular mode is denoted $q_r(t)$ and the instantaneous amplitude of that mode is denoted $Q_r(t)$, i.e. $q_r(t) = \mathrm{Re}\left[Q_r(t)\exp\left(\mathrm{i}\omega_{\mathrm{d}}(t)\right)\right]$ where $\omega_d(t)$ is the instantaneous damped natural frequency.

3 Application to Mass-Spring problem

The proposed methods were first validated on a simple mass-spring system with three discrete Iwan joints, which is shown in the figure below.

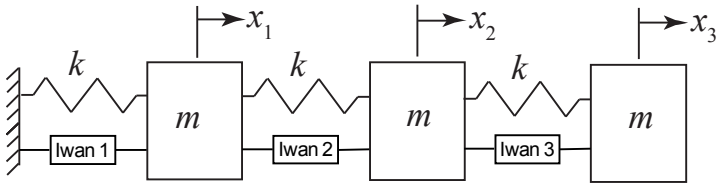

Figure 3: Schematic of the 3DOF system that was used to test the proposed methods.

The parameters of the system were m = 10 kg, k = 5 N/m, and the linear damping matrix was selected based on the mass and the linear springs alone so that $\mathbf{C} = 0.002(\mathbf{M}+\mathbf{K})$. The parameters of the Iwan joints are given in Table 1, and were chosen to assure that each joint had a distinct character. Note, that with these parameters the eigenvalue problem in Eq. (3) becomes the following, and this was solved to obtain the mode shapes that were used to define the static loads in Eq. (10).

$$\left[\left(\left(\begin{bmatrix}10 & -5 & 0\\ -5 & 10 & -5\\ 0 & -5 & 5\end{bmatrix}+\begin{bmatrix}9 & -4 & 0\\ -4 & 7 & -3\\ 0 & -3 & 3\end{bmatrix}\right)\frac{N}{m}-\omega_{0r}{}^{2}\begin{bmatrix}10 & 0 & 0\\ 0 & 10 & 0\\ 0 & 0 & 10\end{bmatrix}kg\right)\boldsymbol{\varphi}_{0r}=0\right] \tag{16}$$

Iwan Joint	Discrete Iwan Joint Parameters			
	F_S	K_T	χ	β
1	10	5	–0.5	0.1
2	1	4	–0.2	0.01
3	100	3	–0.8	1

Table 1: Iwan parameters of the three joints shown in Fig. 3.

Static loads were then applied at 20 amplitudes that were logarithmically spaced between α=0.001 and α=1000 and the quasi-static response was computed and stored at N_α=25 load levels that were linearly spaced between $[0,\alpha]$, to obtain load curves such as that shown in Fig. 1. (The analysis was repeated using N_α=100 and the resulting frequencies changed by less than 1e-14 percent and the damping ratios by less than 1 percent of their values when N_α=25.)

The estimated damping ratios and natural frequencies for the first three modes of vibration are shown in Figs. 4-5. In each plot the parameters estimated using the quasi-static approach are shown with black markers. The plots also show the natural frequency and damping ratio estimated from three transient responses using the approach outlined in Sec. 2.3. Specifically, the transient response of the system with the three nonlinear joints was computed using the Newmark method where the excitation was a 0.1 second long half-sine impulse that was applied: 1) in the shape of the mode in question as given in Eq. (15) (denoted "Modal Force"), 2) to the 3rd mass (denoted x_3), 3) to the 2nd mass (denoted x_2). Then the response was modal filtered, band-pass filtered and processed as explained in Sec. 2.3. In order to

compare with the quasi-static results, which did not include the effect of the linear damping matrix[†], the linear damping ratios $\zeta_{0,1}$=0.00255, $\zeta_{0,2}$=0.00153, $\zeta_{0,3}$=0.00155 were subtracted from the damping estimated by the Hilbert transform.

In each figure, the bottom pane shows the ratio of the displacement amplitude of the mode in question (denoted Q_r) to that of each of the other modes (denoted Q_j) due to the quasi-static loading in Eq. (10). For example, Fig. 4(c) shows the displacement of modes 2 and 3 relative to that of mode 1, and for consistency Q_1/Q_1 is also shown, which is always equal to unity.

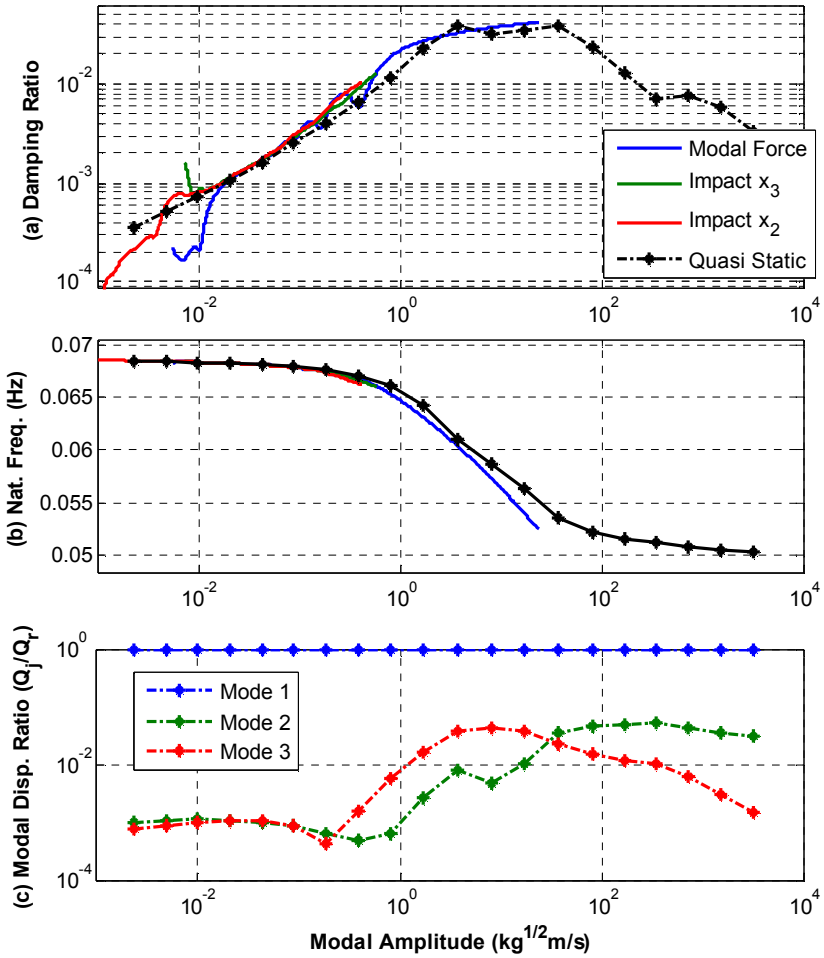

Figure 4: Modal parameters for Mode 1 estimated using the proposed quasi-static approach. (a) and (b) also show the parameters estimated from three transient responses.

Discussion

At low amplitudes the damping estimated by the Hilbert transform becomes noisy, presumably due to end effects of the FFT. The quasi-static approach does not suffer from this problem and seemed to produce reliable damping estimates down below a damping ratio of 0.01%. Below this point material damping would most likely begin to dominate for any real structure. At higher amplitudes the damping begins to increase, initially in a power-law fashion (i.e. the log of the damping increases linearly with the log of the

[†] It was necessary to include a linear damping matrix when computing the transient response, otherwise the response would not decay when the amplitude became low (so that the joint was not active) and this would contaminate the Hilbert Transform since it is based on an FFT.

amplitude) as observed in [6] and [7], and the frequency begins to decrease very slightly. This suggests that each mode could be well described by a modal Iwan model as was used in [6] and [7]. The damping becomes as large as 1% or more, which is an increase of about an order of magnitude from the low-level material damping that was assumed for the system.

At higher amplitudes the damping reaches a maximum and the frequency begins to drop precipitously, signaling the beginning of macro-slip. It is interesting to note that the point at which this occurs is closely aligned with the point at which the other modes begin to be significantly excited in the quasi-static responses. For example, Fig. 4(c) shows that at low amplitudes modes 2 and 3 respond 1000 times less than mode 1 to the static force. However, as the modal velocity amplitude approaches 0.1 $kg^{1/2}$ m/s the response of these modes approaches 5% of that of mode 1 and the system transitions to macro-slip. If the force of interest excites these high amplitudes then it would not be wise to use an uncoupled modal model.

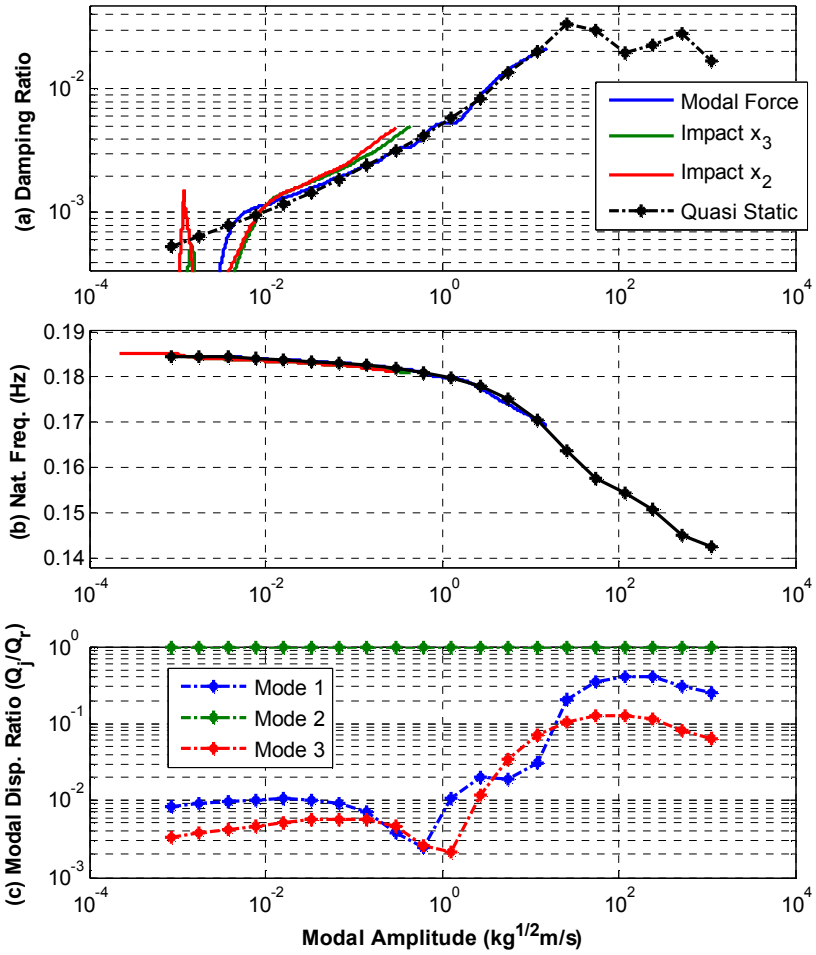

Figure 5: Modal parameters for Mode 2 estimated using the proposed quasi-static approach. (a) and (b) also show the parameters estimated from three transient responses.

It is also worth noting that, although the damping predicted by the quasi-static approach generally agrees very well with that computed from a transient response when a single mode was excited (i.e. the curves denoted "Modal Force"), the impacts at points 2 and 3 sometimes produced noticeably different damping. For example, for mode 2 at amplitudes above 0.1 $kg^{1/2}$ m/s. Above this point the damping in those trials differs by as much as 20-30% from the damping due to a modal force. This indicates that there is some error in approximating the system with three uncoupled weakly-nonlinear oscillators, as elaborated in

[16]. However, to the extent that the uncoupled modal model is accurate, the quasi-static method does an excellent job of predicting the modal behavior.

In their work, Festjens, Chevallier and Dion [10] implemented a procedure to update the mode shapes of the structure as response amplitude increased. This was not done here and the results obtained seem to be quite satisfactory over the range of amplitudes where micro-slip motion is dominant, so there was no reason to consider changes to the mode shapes. However, the joints in this work are discrete and hence clearly different from the continuous interface studied in that work.

4 Application to a Beam Finite Element Model

The quasi-static method was further evaluated on a structural model of a more realistic system, namely the Sumali Beam [6, 16]. The Sumali Beam consists of two, identical, plate-like beams that overlap and are fastened with four bolts. This work uses the exact same Craig-Bampton reduced order model of the beam that was studied in [16]. The reduced order model was created from a finite element model whose mesh is shown in Fig. 6. The two beams are composed of 8-node hexahedral elements with a linear, elastic, isotropic material model. The Young's Modulus is 248 GPa, the Poisson's ratio is 0.29, and the mass density is 8000 kg/m^3.

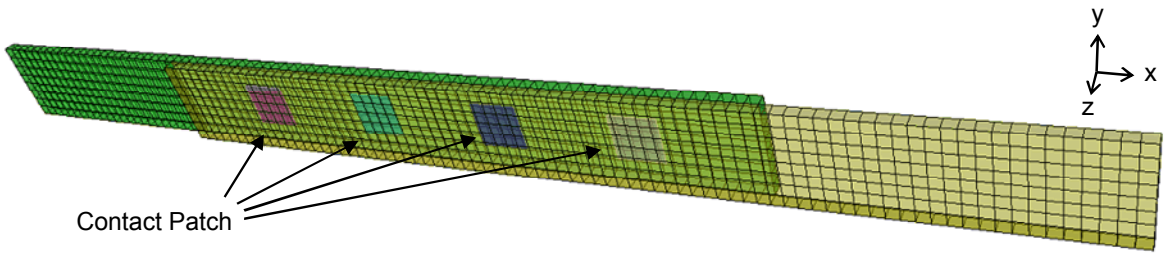

Figure 6: The Sumali beam finite element mesh. The beams are made transparent to reveal the four joint contact patches in between.

The bolts are not modeled, but instead are replaced with whole-joint models. As shown in Fig. 7, a virtual node was assigned to each contact patch on each beam, and the virtual node was constrained to all the nodes within the contact patch using a RBE3 element spider [20], a type of average multi-point constraint. The six degrees of freedom in each virtual node were then tied to those of the opposite virtual node, associated with the opposite contact patch, using a joint model. Each joint model is a collection of rigid constraints, discrete springs, and Iwan elements, and all four joint models in the finite element model are assumed to have the same parameters. The x-translation direction holds a linear spring with stiffness 5.3×10^7 N/m in parallel with a four-parameter Iwan element with parameters $F_S = 30.7$ N, $K_T = 4.73\times10^8$ N/m, $\chi = -0.23$, and $\beta = 0.46$. The y-translational direction has a linear spring with stiffness 5.25×10^8 N/m. All other translational and rotational directions for each virtual node are rigidly constrained except for z-rotation, which is left open with no discrete elements.

The reduced mass and stiffness matrices for the linear beams were assembled using a Craig-Bampton reduction algorithm in Sierra/SD [20]. The details of the reduction are explained in [16]. The matrices were then exported into MATLAB, where the joint models were added. For the following analysis, only the first three free-free elastic modes (first, second, and third bending) were of interest. To apply the quasi-static method to this structure, it was necessary to first apply six constraints to eliminate the rigid body modes.

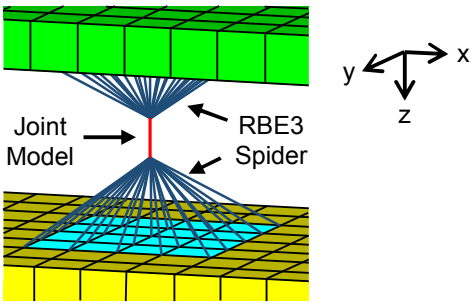

Figure 7: An exploded view of a joint model in the Sumali beam.

The quasi-static response was computed using the methods outlined in Sec. 2.2 to retrieve the modal damping and natural frequency versus amplitude. For the first elastic mode, static loads were applied at 15 amplitudes spaced logarithmically between $\alpha = 0.44$ and $\alpha = 90$ and at another 15 amplitudes spaced logarithmically between $\alpha = 2200$ and $\alpha = 44000$. The spacing was initially continuous between 0.44 and 44000, but the implicit static solver failed to converge at some of the amplitudes in the transition region and so those points were simply skipped. (Future works shall seek to address this issue, but time did not allow it to be pursued here.) Similarly, for the 2nd and 3rd modes the static loads ranged between $\alpha = 0.44$ and $\alpha = 440000$ and the solution was found at 30 points total per mode. At each load amplitude, the quasi-static response was computed at N_α=25 load levels spaced linearly between 0 and α and this load displacement curve was used to derive the modal frequency and damping as described earlier.

Figure 8 shows the damping and natural frequency vs. modal displacement amplitude curves for the three elastic modes. Here, the quasi-static results are juxtaposed with the natural frequency and damping versus amplitude obtained from the transient response as described in [16]. The low-amplitude linear damping ratio of $\zeta_{0r} = 1\times10^{-4}$, which was assigned to all modes for the transient response, was subtracted from the damping data obtained from these responses in order to obtain a valid comparison with the quasi-static results. The results show that the effective damping of each mode increases from below material damping at low amplitude until it exceeds one percent for modes 1 and 3. This is an increase in damping of over two orders of magnitude. The quasi-static algorithm captures this increase in damping exceptionally well, and also captures the (less significant) decrease in each natural frequency.

The quasi-static response was computed in two ways in Fig. 8. After retrieving the static response solution $\mathbf{x}(\alpha)$, the green dot data was retrieved from the hysteresis curve constructed from the modal displacement that was filtered using the low-amplitude mode shapes $\boldsymbol{\varphi}_{0r}$ (as in $q_r(\alpha) = \boldsymbol{\varphi}_{0r}{}^{\mathrm{T}}\mathbf{M}\mathbf{x}(\alpha)$). This is the typical mode of operation as explained earlier. Additionally, to better understand the macroslip behavior of the structure, the filtering was also performed using the high-amplitude mode shapes $\boldsymbol{\varphi}_{\infty r}$ ($q_r(\alpha) = \boldsymbol{\varphi}_{\infty r}{}^{\mathrm{T}}\mathbf{M}\mathbf{x}(\alpha)$) and that result is shown with red triangles. The dynamic response data from [16] was processed in a similar manner. Except for the high amplitude frequency of the 2nd and 3rd modes, filtering with $\boldsymbol{\varphi}_{0r}$ produces quasi-static results that agree remarkably well with the results of the dynamic simulations. Those exceptions correspond to a case where the joint(s) are in the macro-slip regime and so it is not surprising that the micro-slip model is not effective. In most applications of interest the authors expect that the joints will be designed to maintain their integrity, so the forces will not be large enough to induce macro-slip.[‡]

[‡] Of course, there are some applications of interest, such as blast loading of structures, where macroslip may be expected to occur and the methods developed here would need to be extended to account for this.

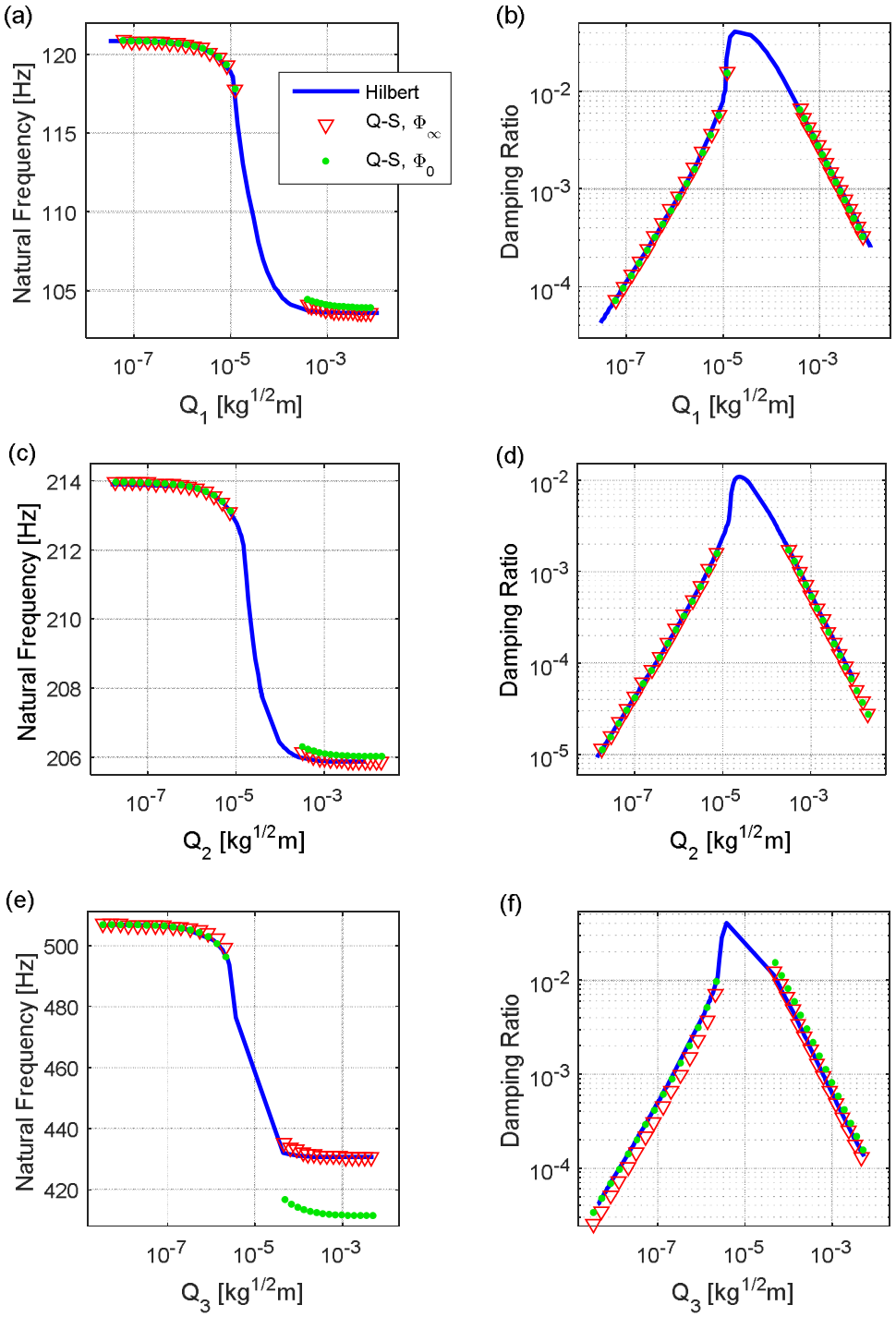

Figure 8: Comparison of the quasi-static (Q-S) method and the Hilbert fitting method for computing (a,c,e) the natural frequency and (b,d,f) the damping vs. modal displacement amplitude for the (a,b) first, (c,d) second and (e,f) third elastic modes.

Considering the excellent agreement obtained, the quasi-static approach is strongly preferred over the dynamic approach. First, while the approach used in [16] was not reviewed in detail here, it is important to note that it was much more complicated and required considerable care to perform all of the signal processing correctly. In contrast, the quasi-static approach requires only a few lines of code and is readily

automated. Second, the quasi-static approach allows for a massive reduction in the computational cost. For the Sumali beam, the time required to complete all of the transient simulations that were needed to produce the frequency and damping versus amplitude curves shown above for all three elastic modes was about 106 minutes. This doesn't include the post-processing, which was non-negligible and required some user interaction. In contrast, the 90 quasi-static responses that were used in the proposed method were computed and post-processed in only 5.5 seconds. This is an astonishing three orders of magnitude reduction in the computational cost. In principle, similar curves could be obtained from a single force-displacement curve for each mode (although with the response stored at additional points along the curve) so the cost could potentially be reduced by another order of magnitude.

5 Conclusions

This work has presented a means of using quasi-static loading to estimate the effective modal natural frequency and damping ratio of each mode of a structure versus amplitude. The proposed approach reduces to that presented by Festjens et al [10] in the case where the entire structure is treated nonlinearly, although this work has presented alternative methods for computing the effective natural frequency and damping. Furthermore, the results presented here suggest that it may not typically be necessary to update the mode shapes to account for slip in the joints. This was theoretically justified by forging a connection between this method and the implicit condensation and expansion method [13].

This method provides a dramatic reduction in computational cost compared to the authors prior approach based on dynamic simulation. This has already been instrumental in allowing the authors to update the parameters of discrete joints in order to bring a finite element model into agreement with experimental measurements. Indeed, this procedure was used on the Sumali beam in order to find the set of discrete joint parameters that were used in these simulations. Those parameters were tuned to approximately reflect the measurements from the beam that were reported in [6]. In prior efforts the authors attempted to do this using the dynamic response alone, yet it proved quite challenging to explore enough of the parameter space in order to find a set of parameters that produced a reasonable agreement with measurements.

It is also important to recall that this method is based on an assumption that the linear modes of a structure remain uncoupled when the displacements are small enough that the structure remains in the micro-slip regime. A significant body of work is beginning to develop that supports this approach when modeling realistic structures [6, 7, 16]. However, there are certainly cases where this assumption does not produce acceptable accuracy. For example, in [16] the authors show that noticeable modal coupling can be observe in the response of the finite element model of the Sumali beam when an impulse is applied at various discrete points on the model. When the response is projected onto the linear modes this causes an apparent error in the damping predictions (because modal coupling was neglected). To date the authors have found these errors to be relatively small, but for some applications it may certainly prove important to extend this approach to account for coupling between modes.

Acknowledgements

This work was supported by Sandia National Laboratories. Sandia is a multi-program laboratory operated by Sandia Corporation, a Lockheed Martin Company, for the United States Department of Energy's National Nuclear Security Administration under Contract DE-AC04-94AL85000. The authors wish to thank Randal L. Mayes for his insights and encouragement to pursue this work.

References

[1] A. A. Ferri, "Friction damping and isolation systems," *Journal of Mechanical Design, Transactions of the ASME,* vol. 117 B, pp. 196-206, 1995.

[2] D. J. Segalman, D. L. Gregory, M. J. Starr, B. R. Resor, M. D. Jew, J. P. Lauffer, and N. M. Ames, "Handbook on Dynamics of Jointed Structures," Sandia National Laboratories, Albuquerque, NM 871852009.

[3] S. Bograd, P. Reuss, A. Schmidt, L. Gaul, and M. Mayer, "Modeling the dynamics of mechanical joints," *Mechanical Systems and Signal Processing,* vol. 25, pp. 2801-2826, 2011.

[4] E. P. Petrov and D. J. Ewins, "Analytical Formulation of Friction Interface Elements for Analysis of Nonlinear Multi-Harmonic Vibrations of Bladed Disks," *Journal of Turbomachinery,* vol. 125, pp. 364-371, 2003.

[5] H. Festjens, G. Chevallier, and J. L. Dion, "Nonlinear model order reduction of jointed structures for dynamic analysis," *Journal of Sound and Vibration,* vol. 333, pp. 2100-2113, 2014.

[6] B. Deaner, M. S. Allen, M. J. Starr, D. J. Segalman, and H. Sumali, "Application of Viscous and Iwan Modal Damping Models to Experimental Measurements From Bolted Structures," *ASME Journal of Vibrations and Acoustics,* vol. 137, p. 12, 2015.

[7] D. R. Roettgen and M. S. Allen, "Nonlinear characterization of a bolted, industrial structure using a modal framework," *Mechanical Systems and Signal Processing,* vol. Accepted Nov. 2015, 2015.

[8] R. C. Flicek, D. A. Hills, J. R. Barber, and D. Dini, "Determination of the shakedown limit for large, discrete frictional systems," *European Journal of Mechanics, A/Solids,* vol. 49, pp. 242-250, 2015.

[9] M. Davies, J. R. Barber, and D. A. Hills, "Energy dissipation in a frictional incomplete contact with varying normal load," *International Journal of Mechanical Sciences,* vol. 55, pp. 13-21, 2012.

[10] H. Festjens, G. Chevallier, and J.-L. Dion, "A numerical tool for the design of assembled structures under dynamic loads," *International Journal of Mechanical Sciences,* vol. 75, pp. 170-177, 2013.

[11] H. Festjens, G. Chevallier, and J.-L. Dion, "A numerical quasi-static method for the identification of frictional dissipation in bolted joints," in *ASME 2012 International Design Engineering Technical Conferences and Computers and Information in Engineering Conference, IDETC/CIE 2012, August 12, 2012 - August 12, 2012*, Chicago, IL, United states, 2012, pp. 353-358.

[12] R. W. Gordon and J. J. Hollkamp, "Reduced-order Models for Acoustic Response Prediction," Air Force Research Laboratory, AFRL-RB-WP-TR-2011-3040, Dayton, OH2011.

[13] J. J. Hollkamp and R. W. Gordon, "Reduced-order models for nonlinear response prediction: Implicit condensation and expansion," *Journal of Sound and Vibration,* vol. 318, pp. 1139-1153, 2008.

[14] M. I. McEwan, J. R. Wright, J. E. Cooper, and A. Y. T. Leung, "A Combined Modal/Finite Element Analysis Technique for the Dynamic Response of a Non-Linear Beam to Harmonic Excitation," *Journal of Sound and Vibration,* vol. 243, pp. 601-624, 2001.

[15] D. J. Segalman, "A Four-Parameter Iwan Model for Lap-Type Joints," *Journal of Applied Mechanics,* vol. 72, pp. 752-760, September 2005.

[16] R. Lacayo, B. Deaner, and M. S. Allen, "A Numerical Study on the Limitations of Modal Iwan Models for Impulsive Excitations," *ASME Journal of Vibrations and Acoustics,* vol. Planned Submission May 2016, 2016.

[17] R. L. Mayes, B. R. Pacini, and D. R. Roettgen, "A Modal Model to Simulate Typical Structural Dynamic Nonlinearity," presented at the 34th International Modal Analysis Conference (IMAC XXXIV), Orlando, Florida, 2016.

[18] M. Eriten, M. Kurt, G. Luo, D. Michael McFarland, L. A. Bergman, and A. F. Vakakis, "Nonlinear system identification of frictional effects in a beam with a bolted joint connection," *Mechanical Systems and Signal Processing,* vol. 39, pp. 245-264, 2013.

[19] G. Masing, "Eigenspannungen und verfestigung beim messing (self stretching and hardening for brass)," presented at the 2nd Int. Congress for Applied Mechanics, Zurich, Switzerland, 1926.

[20] G. M. Reese, "Sierra Structural Dynamics–User's Notes," Sandia National Laboratories, Albuquerque, NM2015.